Assessing the Temporal Consistency of Intra-Urban Surface Thermal Patterns in Satellite LST Time Series: A Case Study of Zagreb, Croatia

Sanja Šamanović, Olga Bjelotomić Oršulić, Vlado Cetl, Danko Markovinović

Department of Geodesy and Geomatics, University North, Jurja Križanića 31b, 42000 Varaždin, Croatia –
(sasamanovic, oborsulic, vcetl, dmarkovinovic)@unin.hr

Keywords: Landsat, land surface temperature, urban thermal patterns, trend analysis, NDVI, NDBI

Abstract

Urban surface warming is often investigated using satellite-derived land surface temperature (LST), but short multi-year time series are difficult to interpret because of interannual variability, limited cloud-free observations, and heterogeneous surface characteristics. This study proposes a practical framework for assessing the temporal consistency and multi-indicator coherence of intra-urban thermal patterns using Landsat observations. The analysis was conducted for Zagreb using Landsat 8/9 Collection 2 Level 2 data for the summers of 2015–2024. Annual composites of LST, the Normalized Difference Vegetation Index (NDVI), and the Normalized Difference Built-up Index (NDBI) were aggregated to 218 local committees as intra-urban spatial units. LST trends were estimated using linear regression, Sen’s slope, and the Mann–Kendall test, while changes in surface characteristics were analysed by comparing the initial and final periods. Results show a widespread increase in summer LST across Zagreb, with an average linear trend of approximately 0.21 °C yr⁻¹ and maximum Sen’s slope values of about 0.35–0.36 °C yr⁻¹. Although the statistical significance of the Mann–Kendall test was limited by the ten-year time series, 216 of 218 local committees showed positive ΔLST values, with an average increase of 1.80 °C. ΔLST was negatively associated with ΔNDVI and positively associated with ΔNDBI. The workflow integrates multi-year Landsat composites, cloud-based processing, and open tools for spatial and statistical analysis, providing a practical framework for interpreting temporally consistent intra-urban surface thermal patterns in complex urban environments.

1. Introduction

Urban areas are increasingly exposed to heat stress due to climate change, land-use change, and the expansion of impervious surfaces. Satellite remote sensing enables these processes to be monitored, particularly through land surface temperature (LST). Landsat data are especially useful in this context because they allow surface thermal patterns within cities to be analysed at a spatial resolution suitable for comparing different urban units. This study analyses Landsat-derived intra-urban surface thermal patterns and their temporal consistency across 218 local committees in Zagreb.

The study focuses on intra-urban surface temperature dynamics at the level of local committees within the City of Zagreb. Although Landsat-derived LST is widely used in surface urban heat island research, multi-year LST patterns are not always straightforward to interpret. Annual values may be influenced by atmospheric conditions, the availability of cloud-free observations, seasonal variability, surface moisture, and meteorologically anomalous years. Consequently, warming signals observed in short satellite time may reflect short-term variability in addition to persistent surface thermal patterns.

To address this issue, the study applies a reproducible geospatial workflow based on Landsat 8/9 observations for the period 2015–2024. Annual summer composites of LST are analysed together with NDVI and NDBI. The workflow includes linear trend estimation, Sen’s slope analysis, the Mann–Kendall test, consistency analysis across sub-periods, analysis of interannual differences, and assessment of long-term change. This approach makes it possible to evaluate whether the observed changes are consistent, spatially differentiated, and associated with indicators of vegetation and built-up surfaces.

The case study focuses on Zagreb, a city with a heterogeneous urban structure, including densely built residential areas, neighbourhoods on the slopes of the mountain, urban green spaces, and peri-urban zones. The study combines complementary trend and consistency analyses to evaluate whether intra-urban thermal patterns remain directionally coherent across multiple indicators and analytical approaches. This methodological framework provides a practical approach for interpreting satellite-derived intra-urban thermal signals in short Landsat time series. The contribution of this study lies in combining multi-year Landsat LST composites with complementary trend estimates, non-parametric testing, and changes in NDVI and NDBI to support a more comprehensive interpretation of intra-urban surface thermal patterns at the local administrative scale.

The study aims to assess whether LST patterns at the level of local committees in Zagreb show a consistent warming tendency during the 2015–2024 period. In addition, the agreement between complementary trend-analysis methods is evaluated and the relationship between interannual LST changes and changes in NDVI and NDBI is examined.

2. Related Work

LST is widely used to analyse intra-urban surface thermal patterns. It provides spatially continuous information on temperature differences within cities. Satellite-based LST studies have therefore become an important part of urban climatology, but their interpretation remains affected by spatial heterogeneity, temporal variability, and limited comparability between studies (Zhou et al., 2019; Kara and Yavuz, 2025). Previous research has consistently shown that LST is negatively associated with vegetation indicators and positively associated with built-up or impervious surface indicators (Guha et al., 2018; Lu et al., 2021; Morabito et al., 2021; Naserikia et al., 2022). These relationships reflect the contrasting thermal behaviour of vegetated and urbanized surfaces. Broader surface thermal patterns are also influenced by urban expansion, land-cover configuration, and urban morphology (Du et al., 2024; Bai et al., 2025; Wang et al., 2024).

https://doi.org/10.5194/isprs-archives-L-4-W1-2026-259-2026 | © Author(s) 2026. CC BY 4.0 License.

LST-based analyses should be distinguished from conventional urban–rural assessments of urban heat island intensity, as they describe surface temperature patterns rather than near-surface air-temperature conditions (Sheng et al., 2017; Marando et al., 2022). For this reason, the spatial and conceptual definition of the analysed units is important. This is also emphasized by the Local Climate Zone approach (Das and Das, 2020; He et al., 2024). In Zagreb, previous Landsat-based studies have shown that green and forested areas generally have lower LST, while built-up areas show higher values (Krtalić et al., 2020; Seletković et al., 2023). Recent Croatian research has also addressed surface and atmospheric heat, 3D urban morphology, and multi-year LST changes in Zagreb (Krsnik, 2024; Bečić and Gašparović, 2025; Šamanović et al., 2026).

Despite this body of work, less attention has been paid to the temporal consistency of Landsat-derived intra-urban surface thermal patterns. This is especially relevant for shorter observation periods. Landsat LST analyses are constrained by revisit period, cloud cover, and the representativeness of available cloud-free scenes. Observed trends may also depend on interannual variability, spatio-temporal resolution, and the selected statistical method (Lu et al., 2021; Halder et al., 2022; Šamanović et al., 2025). Trend methods such as linear regression, the Mann–Kendall test, and Sen's slope are commonly used in this context (Panwar et al., 2018; Zhang et al., 2023). In this study, these methods are combined to evaluate the directional consistency and magnitude of LST change at the level of local committees in Zagreb.

3. Study Area

The research was conducted in the City of Zagreb, the capital and largest urban centre of the Republic of Croatia. Zagreb is in northwestern Croatia, between the southern slopes of Medvednica and the plain of the Sava River. This spatial position, together with its heterogeneous urban structure, contributes to pronounced differences in land cover, built-up density, vegetation distribution, and surface thermal conditions. The city includes a densely built historic core, residential areas developed during different phases of urban development, industrial and commercial zones, larger green areas, and peri-urban spaces (City of Zagreb and Institute for Physical Planning of the City of Zagreb, 2025).

Due to such spatial diversity, Zagreb is suitable for the analysis of intra-urban surface temperature patterns. Previous research has shown that built-up and impervious areas in Zagreb generally exhibit higher LST values, whereas urban forests, parks, and other green areas have lower surface temperatures (Seletković et al., 2023). Recent research, combining mobile air temperature measurements and satellite-derived surface temperature indicators, further shows that Zagreb's heat load can be analysed at multiple spatial and methodological levels (Žgela et al., 2024). This supports the focus of this study on Landsat-derived surface thermal patterns, that is, on the spatial distribution of LST, rather than on the calculation of the classical urban–rural intensity of the atmospheric urban heat island.

The analysis was conducted at the level of 218 local committees of the City of Zagreb, the lowest units of local self-government (Figure 1). This level enables a more detailed interpretation than the level of the entire city or city districts, while at the same time avoiding the excessive fragmentation characteristic of a purely pixel-based analysis. The boundaries of the local committees were obtained from the open spatial data of the City of Zagreb available through the ZG Geoportal (ZG Geoportal, 2026).

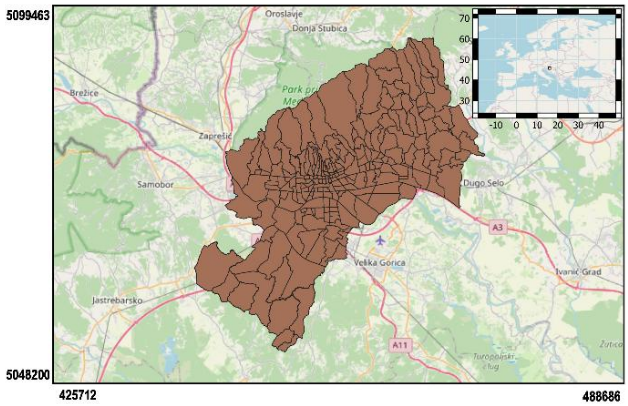

Figure 1. The location of the analysed local committees shown in brown within the City of Zagreb, including an overview map of the study area within the broader European context.

4. Methodology and Results

4.1 Data and Spatial Units

The study used satellite data from the Landsat 8 and Landsat 9 missions, Collection 2 Level 2, accessed through the Google Earth Engine platform. Landsat Collection 2 Level 2 products include surface reflectance and land surface temperature, which makes them suitable for a combined analysis of LST and spectral indices.

The processing workflow combined Google Earth Engine for satellite data filtering, quality masking, and annual composite generation, QGIS for spatial data handling, inspection, and cartographic preparation, and R for statistical analysis and visualization. The complete processing and analytical workflow are summarized in Figure 2.

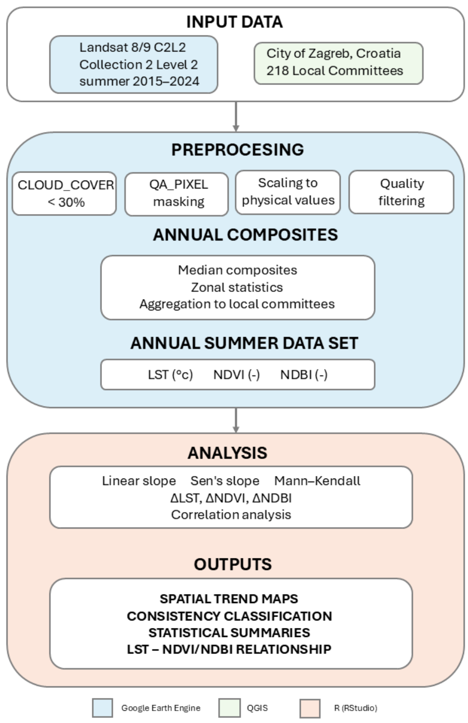

Figure 2. Overview of the reproducible geospatial workflow

Local committee polygons were used as the spatial units for GIS-based aggregation of the annual raster outputs. Individual local committees may contain heterogeneous land-cover compositions, vegetation structures, and built-up characteristics and therefore should not be interpreted as climatically homogeneous units. They were used as practical administrative spatial units for intra-urban aggregation and comparison. Although Google Earth Engine was used as a cloud-based geospatial processing platform, the workflow relies on open satellite data, open-source desktop GIS tools, and reproducible analytical steps. The same processing logic could be transferred to open or interoperable Earth observation environments, such as openEO or STAC-based platforms, provided that equivalent Landsat Collection 2 Level 2 data and quality-mask information are available.

Landsat data were selected because they provide a multi-year record of thermal and multispectral observations, enabling the analysis of changes in LST and related spatial patterns at the urban scale. The temporal scope of the analysis covered the period from 2015 to 2024. For each year, the summer period from 1 June to 31 August was extracted, since surface temperature differences between urbanized, vegetated, and other surface types are most pronounced during this part of the year. The analysis included Landsat scenes that spatially covered the study area and had less than 30% cloud cover according to the CLOUD_COVER metadata field.

4.2 Preprocessing and Calculation of Annual Composites

Before calculating LST and spectral indices, Landsat data preprocessing was performed. Unreliable pixels were removed using the QA_PIXEL band, which in Landsat Collection 2 products contains pixel quality information. Pixels flagged as clouds, cloud shadows, cirrus, dilated clouds, and snow were excluded from the analysis. This reduced the influence of atmospheric disturbances and erroneous values on the results.

LST was calculated from the ST_B10 band. The values were scaled according to the factors for Landsat Collection 2 Level 2 products and converted from Kelvin to degrees Celsius. For each year, an annual summer LST composite was generated by calculating the median of all available and masked Landsat scenes for the period from 1 June to 31 August. The median was used to reduce the influence of individual extreme values, residual atmospheric disturbances, and anomalous scenes. A potential limitation is that median composites may smooth short-duration heat events and reduce the influence of short-term thermal extremes.

For the same period, the spectral indices NDVI and NDBI were also calculated to relate changes in LST to vegetation cover and the degree of built-up development. Before calculating the indices, the optical Landsat Surface Reflectance bands were scaled according to the factors for Collection 2 Level 2 products. NDVI was calculated from bands SR_B5 and SR_B4, while NDBI was calculated from bands SR_B6 and SR_B5. NDVI was used as an indicator of vegetation presence and density, whereas NDBI was used as an indicator of built-up and sparsely vegetated surfaces.

4.3 Zonal Statistics and Time Series Generation

For each local committee and each year, mean values of LST, NDVI, and NDBI were calculated. This produced annual time series of summer land surface temperature, the vegetation index, and the built-up index for 218 local committees of the City of Zagreb for the period 2015–2024. Zonal statistics were calculated on the 30 m Landsat Collection 2 Level 2 grid. The polygons of the local committees were used as spatial zones, and the mean value of the corresponding raster was calculated for each zone.

Table 1 presents an excerpt from the summer LST, NDVI, and NDBI time series by local committee. The LST column denotes the mean summer LST for a given local committee and year, expressed in °C. The NDVI and NDBI columns denote the mean summer values of the vegetation index and the built-up index, respectively. The valid_pixels column denotes the number of valid pixels included in the calculation of the mean values after masking invalid observations, while total_pixels denotes the total number of reference pixels with a spatial resolution of 30 m within the boundary of each local committee. The image_count column indicates the number of Landsat scenes included in the generation of the annual summer composite.

JMS_MB	MO	year	LST	NDVI	NDBI	valid pixels	total pixels	image count
48585	Brezovica	2015	34.99	0.63	-0.17	19643	19643	7
48593	Demerje	2015	31.89	0.76	-0.29	16927	16927	7

Table 1. Excerpt from the annual summer LST, NDVI, and NDBI time series for local committees of the City of Zagreb, 2015–2024.

For linking the tabular and spatial data, the official local committee code JMS_MB was used. Table 1 presents a combined excerpt from the complete datasets for LST, NDVI, and NDBI. The complete datasets each contain 2,180 records, corresponding to annual values for 218 local committees over the ten-year period. In the original results, LST was stored in a separate dataset, while NDVI and NDBI were stored together. Differences between valid pixels and total pixels, where present, result from the masking of invalid observations. The number of Landsat scenes used to generate the annual summer composites varies among years, depending on the availability of valid observations after filtering and masking, and ranges from 4 to 16.

4.4 Interannual Variability of LST

Before analysing long-term trends, the interannual variability of LST should be considered as an important source of differences among annual summer composites. These differences may be influenced by meteorological conditions at the time of image acquisition, the availability of valid Landsat observations after cloud masking, and the spatial heterogeneity of urban surfaces. Figure 3 shows the distribution of mean summer LST values by local committee in the City of Zagreb for the period 2015–2024. Each box represents the distribution of values for a given year, while the points represent individual local committees.

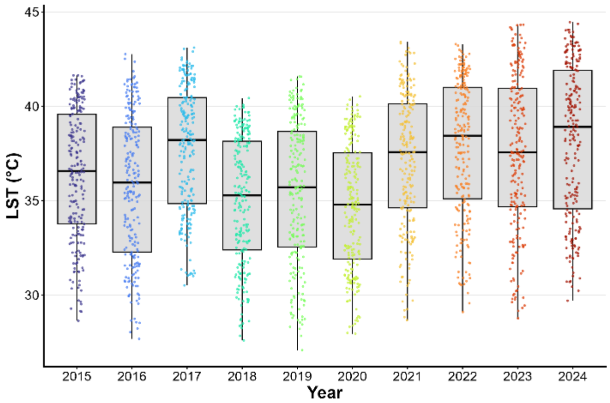

Figure 3. Interannual variability of summer LST by local committee in the City of Zagreb, 2015–2024. Box plots show the distribution of mean summer LST values by year, while points represent individual local committees; colours distinguish individual years.

Pronounced interannual variability is evident, with lower values and lower medians occurring particularly in 2016, 2018, 2019, and 2020. Higher values were recorded in 2017 and in the final part of the analysed period, particularly in 2022 and 2024. The year 2024 stands out with the highest median summer LST, indicating markedly warm surface conditions across a large proportion of local committees.

Due to the pronounced interannual variability, the main conclusions in the following sections are not based on individual years, but on time series, trends, and a comparison of the initial and final periods. Landsat LST time series are useful for monitoring spatio-temporal patterns of surface temperature, but their interpretation may be sensitive to image availability and observation conditions.

4.5 Trend Magnitude and Spatial Consistency of LST Patterns

After generating the annual summer LST composites and calculating zonal statistics, the change in summer LST was estimated separately for each local committee for the period 2015–2024. In this study, stability is interpreted as consistency in the direction and spatial pattern of LST change across complementary indicators, rather than as statistical significance alone. As an initial trend estimate, a linear regression model was applied, in which the mean annual summer LST value was used as the dependent variable and year as the independent variable:

$$LST_t = \alpha + \beta t + \varepsilon_t \quad (1)$$

where LST_t is the mean summer LST in year t, α is the regression intercept, $\beta$is the annual trend in LST change, and ε_t is the residual error. The coefficient β was interpreted as the average annual change in surface temperature, expressed in °C yr^{-1}.

The results show that a positive summer LST trend was recorded in most local committees. The spatial distribution of the linear trend is shown in Figure 4. More pronounced increases occur in the central and southern parts of the city. Lower trend values occur in peripheral and less urbanized local committees, especially in the foothill area of Medvednica and in the southern and northeastern urban margins (Figure 4a). The histogram in Figure 4b further shows that the distribution is shifted towards positive values, with an average trend of approximately 0.21 °C yr^{-1}, while the highest values approach 0.34 °C yr^{-1}.

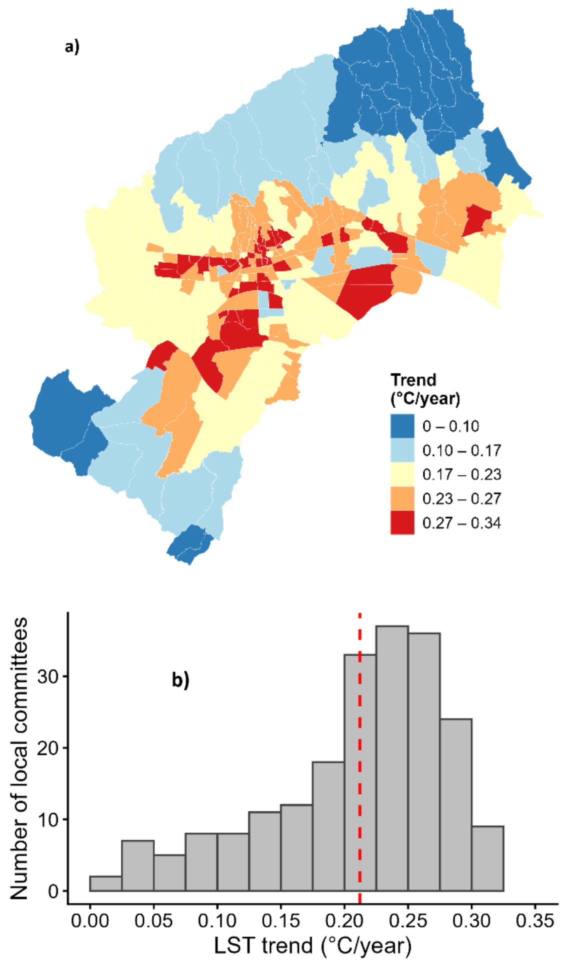

Figure 4. Spatial distribution of the linear trend in summer LST by local committee in the City of Zagreb, 2015–2024 (a) and the histogram shows the distribution of linear trends, while the dashed line indicates the mean trend value (b).

For an additional consistency check of the results, Sen's slope of summer LST was calculated for each local committee. Unlike the classical linear regression slope, Sen's slope is a non-parametric trend estimator based on the median of all pairwise changes in values over time. It is less sensitive to individual extreme years or deviations in the time series.

Sen's slope values are expressed in °C yr^{-1} and represent the average annual change in summer LST during the period 2015–2024. The spatial distribution of Sen's slope is shown in Figure 5. The spatial pattern is broadly consistent with the linear trend, although local differences between the two classifications are visible. Higher values are again concentrated in the southern, southwestern, and central urbanized parts of the city, while lower values are more frequent in northern and peripheral areas (Figure 5a). Slightly negative values in the lowest class were interpreted as a very weak or nearly consistent trend rather than as pronounced cooling.

The histogram in Figure 5b further shows that most local committees fall within the positive trend range. Slightly negative values occur only in a small number of local committees, while values close to zero are weakly represented. The distribution is concentrated mainly around 0.20–0.30 °C yr^{-1}, with the highest

This contribution has been peer-reviewed.
https://doi.org/10.5194/isprs-archives-L-4-W1-2026-259-2026 | © Author(s) 2026. CC BY 4.0 License.

frequency around approximately 0.22–0.25 °C yr⁻¹. The mean value, marked by the dashed line, is slightly above 0.20 °C yr⁻¹, while the highest values approach 0.35–0.36 °C yr⁻¹. This distribution indicates that positive Sen’s slope values dominate across the analysed local committees.

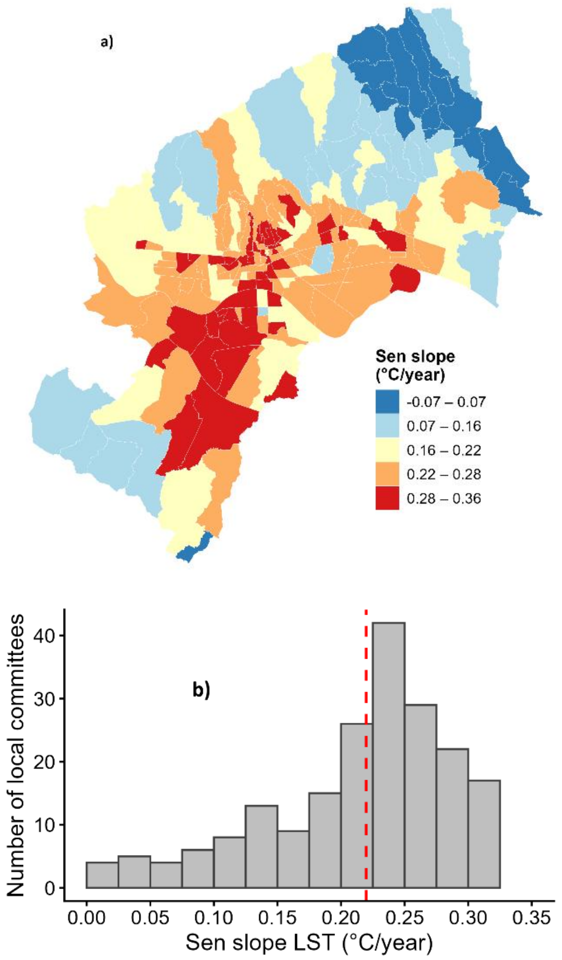

Figure 5. Spatial distribution of Sen’s slope trend in summer LST by local committee in the City of Zagreb, 2015–2024 (a) and the histogram shows the distribution of Sen’s slope trends, while the dashed line indicates the mean trend value (b).

Although the linear trend and Sen’s slope maps show broadly similar spatial patterns, local differences between the two trend estimates are visible. Agreement between the methods was additionally evaluated through a direct comparison of the estimated slopes (Figure 6). This comparison was used to assess the agreement between two complementary trend-analysis methods. The linear slope provides a simple and directly interpretable estimate of the average annual change in LST in °C yr⁻¹, while Sen’s slope provides a more robust estimate that is less sensitive to individual extreme years and deviations in the time series.

The results indicate a strong agreement between the two trend estimates, with a Pearson correlation coefficient of $r = 0.875$. This suggests that the identified spatial pattern of summer LST change is consistent across the applied trend-analysis methods and is not dependent on a single trend-estimation approach. This agreement supports the interpretation of the detected LST increase as a directionally consistent surface thermal signal that is recurrently detected across complementary trend-estimation approaches.

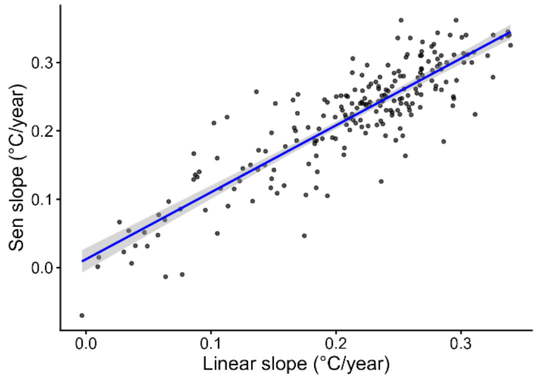

Figure 6. Agreement between linear regression slope and Sen’s slope for summer LST trends by local committee, 2015–2024. Each point represents one local committee; the fitted line indicates the relationship between the two trend estimates.

4.6 Statistical Support for the Surface Warming Signal

The Mann–Kendall trend test was used to assess the statistical support for a monotonic trend in summer LST, with the p-value and Kendall’s tau coefficient recorded as test indicators. Values with $p < 0.05$ and $\tau > 0$ were classified as statistical support for an increase, values with $0.05 \leq p < 0.10$ and $\tau > 0$ as indicative support for an increase, and all remaining cases as having no statistical support for an increasing trend.

Figure 7 shows the spatial distribution of statistical support for the summer LST trend according to the Mann–Kendall test for the period 2015–2024. Of the 218 local committees, 197 were classified as having no statistical support.

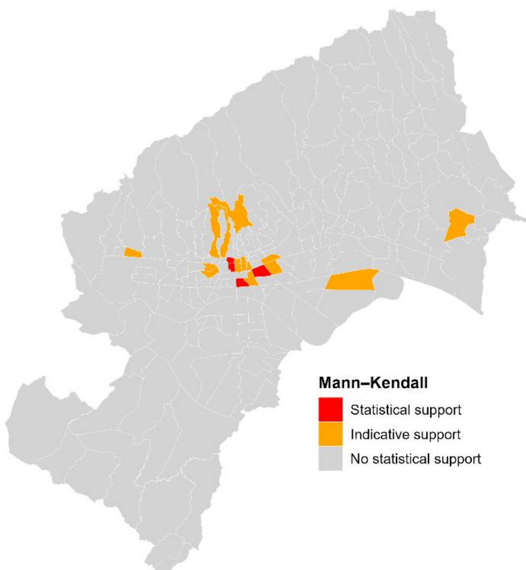

Figure 7. Statistical support for the summer LST trend by local committees of the City of Zagreb according to the Mann–Kendall test, 2015–2024.

A total of 17 local committees were classified as showing indicative support for an increase; these are mainly concentrated in the central urban area, with individual occurrences in the eastern and western more peripheral parts of the city, for example in Resnik and Budenec in the east and Stenjevec – sjever in the west. Four local committees show statistical support for an increase: Kralj Petar Svačić, Cvjetni trg, Kanal, and Trnje.

Although the analysed period includes only ten annual summer observations per local committee, the Mann–Kendall test identified a limited subset of areas showing statistical support for increasing summer LST. This suggests that increasing summer LST is detectable in selected parts of the city, particularly within the central urban area, despite the relatively short time series and expected interannual variability. Part of the observed variability may also reflect broader regional climatic conditions and anomalously warm summers affecting the wider region rather than exclusively local urban-surface processes. The large number of local committees without statistical support should not be interpreted as definitive evidence against warming trends. This outcome likely reflects the limited statistical power associated with short time series, together with the conservative nature of the Mann–Kendall test and pronounced interannual variability. The Mann–Kendall results are interpreted as supplementary evidence regarding the statistical support for warming tendencies, while the magnitude of change is assessed using the linear slope and Sen's slope, expressed in °C yr^{-1}.

4.7 Directional Consistency Classification of Surface Thermal Change

In this study, directional consistency refers to the agreement in the direction of change across complementary trend indicators rather than to statistical stability in a strict time-series sense. To make the assessment of directional consistency explicit, the complementary trend indicators were combined into a directional consistency classification. The classification was based on three indicators: linear slope, Sen's slope, and long-term ΔLST. A local committee was classified as having a consistent positive warming pattern when all three indicators showed a positive direction of change. Since most local committees met this condition, an additional magnitude-based distinction was introduced. A strong consistent warming pattern was assigned when all three indicators were positive and above their city-wide mean values. City-wide mean values were used as practical thresholds for distinguishing stronger warming patterns rather than as statistically derived cut-off values. Local committees with two positive indicators were classified as moderately consistent, whereas those with zero or one positive indicator were classified as weakly consistent or inconsistent. The resulting spatial classification is shown in Figure 8.

The classification shows that 106 local committees (48.6%) were classified as having a strong consistent positive signal, while 108 local committees (49.5%) showed a consistent positive signal. Only three local committees (1.4%) were classified as moderately consistent, and one local committee (0.5%) as weak or inconsistent. In total, 214 of 218 local committees (98.2%) exhibited a consistent positive surface thermal signal across the applied indicators. Spatially, strong positive consistency was concentrated mainly in the central urban area and parts of southern Zagreb, whereas moderately consistent and weak or inconsistent signals occurred only in a limited number of local committees. This indicates that, although formal Mann–Kendall statistical support was limited by the short ten-year time series, the direction of LST change remained broadly consistent across the analysed indicators. The directional consistency classification provides an additional interpretation layer between trend magnitude and formal statistical significance.

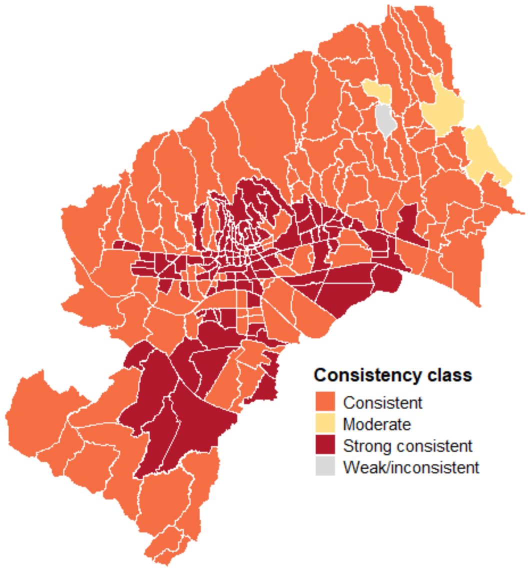

Figure 8. Consistent and magnitude classification of summer LST change by local committee in the City of Zagreb, 2015–2024.

4.8 Relationship Between LST Changes and Changes in NDVI and NDBI

To relate changes in summer LST to changes in surface characteristics, NDVI was included as an indicator of vegetation cover and NDBI as an indicator of built-up and sparsely vegetated surfaces. For each local committee, mean LST, NDVI, and NDBI values were calculated for the initial period 2015–2016 and the final period 2023–2024, after which the differences ΔLST, $\Delta NDVI$, and $\Delta NDBI$ were computed. Two-year averaging was used for the initial and final periods to reduce the influence of anomalous single-year conditions and short-term interannual variability while preserving the temporal contrast between the beginning and end of the analysed period.

The relationships between LST changes and changes in surface indices were examined using linear regression models ($\Delta LST \sim \Delta NDVI$ and $\Delta LST \sim \Delta NDBI$). The relationship between ΔLST and $\Delta NDVI$ is shown in Figure 9a. The regression line has a negative slope, indicating that local committees with a greater decrease in NDVI generally experienced a greater increase in LST. The fitted regression model showed a significant negative relationship between ΔNDVI and ΔLST, indicating that decreases in vegetation cover were associated with increases in LST (slope = −21.40, R^2 = 0.197, p = 6.19 × 10^{-12}).

The opposite pattern is visible in the relationship between ΔLST and $\Delta NDBI$, shown in Figure 9b. The positive slope indicates that local committees with a greater increase in NDBI generally experienced a greater increase in LST. The fitted regression model showed a significant positive relationship between $\Delta NDBI$ and ΔLST (slope = 17.38, $R^2 = 0.099$, $p = 2.14 \times 10^{-6}$). These relationships are consistent with common findings that LST is negatively associated with vegetation indices and positively associated with indicators of built-up land (Guha et al., 2018; Cetin et al., 2024).

https://doi.org/10.5194/isprs-archives-L-4-W1-2026-259-2026 | © Author(s) 2026. CC BY 4.0 License.

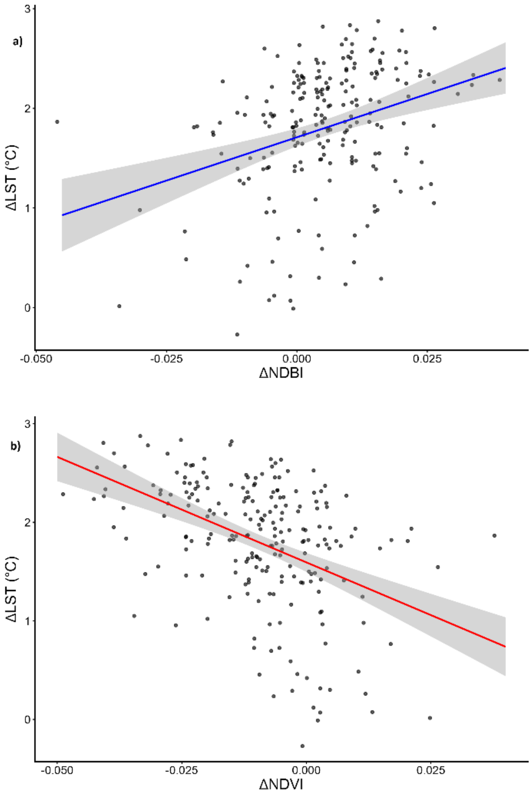

Figure 9. Relationship between ΔLST and changes in NDVI and NDBI by local committees of the City of Zagreb. Panel (a) shows the relationship between ΔLST and $\Delta NDVI$, while panel (b) shows the relationship between ΔLST and $\Delta NDBI$. The red and blue lines represent fitted linear regression lines, and the grey bands indicate confidence intervals.

The comparison of the two models shows that changes in NDVI are more strongly associated with changes in LST than changes in NDBI. Both indices explain only part of the variability in surface temperature change. The relatively low R^2 value indicates that a large proportion of spatial variability in LST remains unexplained. Vegetation cover and built-up areas therefore contribute to spatial differences in warming, but do not fully explain the observed temperature patterns. Other factors may also influence LST dynamics, including urban morphology, building density, surface materials, Local Climate Zone characteristics, anthropogenic heat emissions, and broader climatic conditions.

5. Conclusions

This study assessed the consistency of intra-urban surface thermal patterns in Zagreb using satellite-derived summer LST time series for the period 2015–2024. The analysis was conducted at the level of 218 local committees and combined annual Landsat LST composites, linear regression, Sen's slope, the Mann–Kendall test, long-term ΔLST, and changes in NDVI and NDBI. In this way, the study focused not only on detecting surface warming, but also on evaluating whether the observed spatial patterns were consistent across complementary indicators.

The results indicate a widespread and directionally consistent increase in summer LST across Zagreb, with an average warming trend of approximately 0.21 °C yr^{-1}. The estimated warming magnitude is relatively high compared with long-term regional climate trends and should therefore be interpreted primarily as a Landsat-derived surface-temperature signal rather than as an equivalent atmospheric warming rate. Long-term comparison further showed positive ΔLST values in 216 of 218 local committees, with an average increase of approximately 1.80 °C, indicating that warming was spatially widespread across the study area. The strong agreement between linear regression and Sen's slope ($r = 0.875$) suggests that the identified spatial patterns were not dependent on a single trend-estimation approach and can be interpreted as directionally consistent thermal patterns despite interannual variability.

The Mann–Kendall test provided limited formal statistical support, with only four local committees showing statistically supported increasing trends and 17 showing weak statistical support. This limitation is likely related not only to the short ten-year time series and the use of one annual summer composite per year, but also to interannual variability and limited statistical power. The observed relationships with surface indices were consistent with expectations: ΔLST was negatively associated with ΔNDVI and positively associated with ΔNDBI, although these indices explained only part of the spatial variability in warming.

Landsat-derived LST represents surface rather than near-surface air temperature, and local committees are administrative rather than homogeneous climatic units. Surface thermal patterns derived from satellite observations should not be interpreted as direct measures of human thermal exposure. Nevertheless, the proposed workflow can be transferred to other cities with comparable Landsat coverage and available intra-urban spatial units. Future research should test its applicability to longer harmonized Landsat time series and additional urban-climatic and morphological indicators. The proposed open-data and reproducible workflow provide a practical framework for identifying persistent intra-urban thermal patterns and may support future urban climate assessment in Zagreb and comparable urban environments.

Acknowledgments

The authors acknowledge the financial support of University North through the scientific project "The Influence of the 3D Structure of a City on the Intensity of the Urban Heat Island", project number UNIN-TEH-26-1-4, Varaždin, Croatia (2026).

Data and Code Availability

The Google Earth Engine and R scripts used in this study are available at: https://github.com/SanjaSamanovic/zagreb-foss4g-hiroshima.

References

Bai, Y., Wang, M., Yan, Y., Wang, H., 2025. Exploring the impact of 2D/3D urban morphology on land surface temperature within the diurnal cycle in Tianjin. *Scientific Reports*, 15, 39740. doi.org/10.1038/s41598-025-17849-7.

Bečić, D., Gašparović, M., 2025. Urban heat islands and land-use patterns in Zagreb: A composite analysis using remote sensing and spatial statistics. *Land*, 14(7), 1470. doi.org/10.3390/land14071470.

Cetin, M., Ozenen Kavlak, M., Senyel Kurkcuoglu, M.A., Ozturk, G.B., Cabuk, S.N., Cabuk, A., 2024. Determination of land surface temperature and urban heat island effects with remote sensing capabilities: The case of Kayseri, Türkiye. *Natural Hazards*, 120(6), 5509–5536. doi.org/10.1007/s11069-024-06431-5.

City of Zagreb, City Office for Economy, Environmental Sustainability and Strategic Planning, Institute for Physical Planning of the City of Zagreb, 2025. Amendments and supplements to the Zagreb Spatial Plan 2025 (Izmjene i dopune Prostornog plana Grada Zagreba 2025). City of Zagreb, Zagreb, Croatia.
zagreb.hr/userdocsimages/arhiva/prostorni_planovi/novi%20ppgz/01_ID_PPGZ_2025.pdf (25 May 2026).

Das, M., Das, A., 2020. Assessing the relationship between local climatic zones (LCZs) and land surface temperature (LST): A case study of Sriniketan-Santiniketan Planning Area (SSPA), West Bengal, India. *Urban Climate*, 32, 100591. doi.org/10.1016/j.uclim.2020.100591.

Du, S., Wu, Y., Guo, L., Fan, D., Sun, W., 2024. How does the 2D/3D urban morphology affect the urban heat island across urban functional zones? A case study of Beijing, China. *ISPRS International Journal of Geo-Information*, 13(4), 120. doi.org/10.3390/ijgi13040120.

Guha, S., Govil, H., Dey, A., Gill, N., 2018. Analytical study of land surface temperature with NDVI and NDBI using Landsat 8 OLI and TIRS data in Florence and Naples city, Italy. *European Journal of Remote Sensing*, 51(1), 667–678. doi.org/10.1080/22797254.2018.1474494.

Halder, B., Karimi, A., Mohammad, P., Bandyopadhyay, J., Brown, R.D., Yaseen, Z.M., 2022. Investigating the relationship between land alteration and the urban heat island of Seville city using multi-temporal Landsat data. *Theoretical and Applied Climatology*, 150, 613–635. doi.org/10.1007/s00704-022-04180-8.

He, X., Yuan, Q., Qin, Y., Lu, J., Li, G., 2024. Analysis of surface urban heat island in the Guangzhou-Foshan Metropolitan Area based on local climate zones. *Land*, 13(10), 1626. doi.org/10.3390/land13101626.

Kara, Y., Yavuz, V., 2025. Urban microclimates in a warming world: Land surface temperature (LST) trends across ten major cities on seven continents. *Urban Science*, 9(4), 115. doi.org/10.3390/urbansci9040115.

Krsnik, G., 2024. Is Zagreb green enough? Influence of urban green spaces on mitigation of urban heat island: A satellite-based study. *Earth*, 5(4), 604–622. doi.org/10.3390/earth5040031.

Krtalić, A., Kuveždić Divjak, A., Čmrlec, K., 2020. Satellite-driven assessment of surface urban heat islands in the City of Zagreb, Croatia. ISPRS Annals of the Photogrammetry, *Remote Sensing and Spatial Information Sciences*, V-3-2020, 757–764. doi.org/10.5194/isprs-annals-V-3-2020-757-2020.

Lu, Y., Yue, W., Huang, Y., 2021. Effects of land use on land surface temperature: A case study of Wuhan, China. *International Journal of Environmental Research and Public Health*, 18(19), 9987. doi.org/10.3390/ijerph18199987.

Marando, F., Heris, M.P., Zulian, G., Udías, A., Mentaschi, L., Chrysoulakis, N., Parastatidis, D., Maes, J., 2022. Urban heat island mitigation by green infrastructure in European Functional Urban Areas. *Sustainable Cities and Society*, 77, 103564. doi.org/10.1016/j.scs.2021.103564.

Morabito, M., Crisci, A., Guerri, G., Messeri, A., Congedo, L., Munafò, M., 2021. Surface urban heat islands in Italian metropolitan cities: Tree cover and impervious surface influences. *Science of the Total Environment*, 751, 142334. doi.org/10.1016/j.scitotenv.2020.142334.

Naserikia, M., Hart, M.A., Nazarian, N., Bechtel, B., 2022. Background climate modulates the impact of land cover on urban surface temperature. *Scientific Reports*, 12, 15433. doi.org/10.1038/s41598-022-19431-x.

Panwar, M., Agarwal, A., Devadas, V., 2018. Analyzing land surface temperature trends using non-parametric approach: A case of Delhi, India. *Urban Climate*, 24, 19–25. doi.org/10.1016/j.uclim.2018.01.003.

Schmidt, P., Lawrence, B.T., 2022. Association between land surface temperature and green volume in Bochum, Germany. *Sustainability*, 14(21), 14642. doi.org/10.3390/su142114642.

Seletković, A., Kičić, M., Ančić, M., Kolić, J., Pernar, R., 2023. The urban heat island analysis for the City of Zagreb in the period 2013–2022 utilizing Landsat 8 satellite imagery. *Sustainability*, 15(5), 3963. doi.org/10.3390/su15053963.

Sheng, L., Tang, X., You, H., Gu, Q., Hu, H., 2017. Comparison of the urban heat island intensity quantified by using air temperature and Landsat land surface temperature in Hangzhou, China. *Ecological Indicators*, 72, 738–746. doi.org/10.1016/j.ecolind.2016.09.009.

Šamanović, S., Bjelotomić Oršulić, O., Krajina, T., Markovinović, D., 2025. Tracking urban heat island dynamics using open source tools and free data. *The International Archives of the Photogrammetry, Remote Sensing and Spatial Information Sciences*, XLVIII-4/W13-2025, 217–224. doi.org/10.5194/isprs-archives-XLVIII-4-W13-2025-217-2025.

Šamanović, S., Bjelotomić Oršulić, O., Cetl, V., Krtalić, A., 2026. The influence of three-dimensional urban form on the dynamics of urban thermal patterns: A case study of Zagreb, Croatia. *Land*, 15(5), 693. doi.org/10.3390/land15050693.

Wang, C., Zhang, H., Ma, Z., Yang, H., Jia, W., 2024. Urban morphology influencing the urban heat island in the high-density city of Xi'an based on the local climate zone. *Sustainability*, 16(10), 3946. doi.org/10.3390/su16103946.

Zhang, Q., Feng, T., Wang, M., Yang, G., Lu, H., Sun, W., 2023. A twenty-year assessment of spatiotemporal variation of surface temperature in the Yangtze River Delta, China. *Remote Sensing*, 15(9), 2274. doi.org/10.3390/rs15092274.

Zhou, D., Xiao, J., Bonafoni, S., Berger, C., Deilami, K., Zhou, Y., Frolking, S., Yao, R., Qiao, Z., Sobrino, J.A., 2019. Satellite remote sensing of surface urban heat islands: Progress, challenges, and perspectives. *Remote Sensing*, 11(1), 48. doi.org/10.3390/rs11010048.

ZG Geoportal, 2026. GeoPortal of the Zagreb Spatial Data Infrastructure. City of Zagreb. geoportal.zagreb.hr/ (25 May 2026).

Žgela, M., Lozuk, J., Jureša, P., Justić, K., Popović, M., Boras, M., Herceg-Bulić, I., 2024. Urban heat load assessment in Zagreb, Croatia: A multi-scale analysis using mobile measurement and satellite imagery. *Environmental Monitoring and Assessment*, 196, 410. doi.org/10.1007/s10661-024-12538-w.